Journal of Convex Analysis
Volume 18 (2011), No. 1, 153–172

Continuum Limit of a Double-Chain Model for Multiload Shape Optimization*

Pradeep Atwal
Institut für Angewandte Mathematik, Universität Bonn,
Endenicher Allee 60, 53115 Bonn, Germany
pradeep.atwal@uni-bonn.de

Received: February 15, 2008
Revised manuscript received: July 6, 2009

We compute explicitly the Γ-limit of an energy functional modeling a connected mass-spring double-chain in the limit of small separations. The point masses interact with each other through nearest neighbor potentials that have to be convex and fulfill a growth condition (e.g. modeling harmonic springs). This results in a continuous one-dimensional variational problem whose minimum approximates those of the discrete problem for large N, which is used to numerically compute the deformation under various loadings. In a second step, we use our model to numerically optimize the macroscopic distribution of material strength in the presence of stochastic loads.

1. Introduction

In this paper we consider a shape optimization problem for a one-dimensional periodic microstructure, i.e, we want to numerically optimize the macroscopic distribution of material strength along its length (see for example Allaire [1] or Bucur and Buttazzo [8] for an introduction to shape optimization). The microstructure is a connected mass-spring double-chain with nearest neighbor potentials, which have to be convex and fulfill a growth condition (e.g. modeling harmonic springs) (see Figure 1.1). This can be seen for example as a model for treating a structure composed of a series of struts and joints. Despite the simple design, two numerical problems arise: (i) The solution in the case of compression is not unique (similar to crumpling of paper), and (ii) the grid-fineness of the algorithm is already fixed by the problem, which results in a number of operations of order N to compute the energy for a given configuration. A natural question is whether there is a way to use the periodicity of the structure to reformulate the problem. For a continuous problem like the fine-scale mixture of different materials we would think of homogenization (for example in the framework of H-convergence) to approximate the problem with some effective material (for further details on that topic see Cioranescu and Donato [10] and also [1], [2]). In our case we use Γ-convergence to obtain a limit problem for $N \to \infty$, which yields a transition from a discrete to a continuous model with an effective potential, capturing the behavior of the structure (see Theorem 3.3 and 3.7). This shows that it is not necessary to have detailed information on the microstructure to understand

*This work was supported by the Deutsche Forschungsgemeinschaft through the Schwerpunktprogramm 1253 *Optimization with Partial Differential Equations.*

ISSN 0944-6532 / $ 2.50

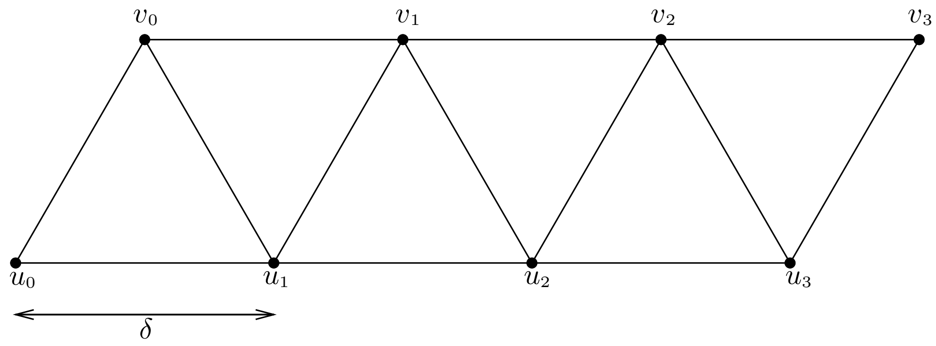

Figure 1.1: Reference configuration of u and v for $N = 3$

the response to macroscopic loads. The resulting continuous one-dimensional variational problem, whose minimum approximates those of the discrete problem for large N, is now the effective problem. The limit model retains the nonlinearity of the discrete problem, which arises even when considering harmonic springs by the nonlinear treatment of rotations. Thus we have decoupled the grid-scale of the original problem and the numerical algorithm and also, as we see later, are able to regularize the problem to make the solution well posed even under compression. This enables us to easily compute the deformation for a given load, which then allows us to use standard numerical methods to solve the shape optimization problem with respect to stochastic loads (see e.g. [3], [5], [16], [11]). This work can be seen as a starting point to study other similar $1\frac{1}{2}$-dimensional problems (e.g. carbon nanotubes). Also it would be interesting to study a different scaling of the energy, in particular in the situation where bending energy plays a role. This could be especially relevant when extended to a higher dimension to study thin plates (see e.g. [14] in that direction).

Let us now go into details and write the problem in a more precise way. We consider the functional

$$\begin{aligned} E_N(\{u_i^N\},\{v_i^N\}) = \delta \sum_{i=0}^{N-1} V\left(\frac{|u_i^N - u_{i+1}^N|}{\delta}\right) + V\left(\frac{|v_i^N - v_{i+1}^N|}{\delta}\right) \\ + V\left(\frac{|u_i^N - v_i^N|}{\delta}\right) + V\left(\frac{|u_{i+1}^N - v_i^N|}{\delta}\right), \end{aligned} \tag{1}$$

where $\{u_i^N\} = \{u_0^N, \ldots, u_N^N\}$ with $u_i^N \in \mathbb{R}^2$ (and the same for $\{v_i^N\}$). The potential V is a convex $C^0([0,\infty),\mathbb{R})$ function with p-growth ($p > 1$), which for convenience henceforth always assumes its minimum value 0 at the point 1. Here p-growth is defined as:

$$c_1|z|^p - c_2 \leq V(z) \leq c_3(1 + |z|^p). \tag{2}$$

One can see E_N as an energy functional modeling the discrete microstructure as pictured in Figure 1.1.

In the following we want to solve two problems:

1. We want to compute the deformation after applying some load in the case of very large N. This corresponds to finding the minimum of the energy functional plus some force term.

2. After introducing the macroscopic design parameter φ, which models the strength of the potential at different points of the structure:

$$E_N(\{u_i^N\},\{v_i^N\}) = \delta \sum_{i=0}^{N-1} \varphi_i \left[V\left(\frac{|u_i^N - u_{i+1}^N|}{\delta} \right) + \dots \right], \tag{3}$$

we want to solve the shape optimization problem of finding the φ, which minimizes the deformation for a given set of forces.

1.1. Notation

Before we compute the Γ-limit of the discrete functional, we parameterize it over the interval $[0,1]$. Define

$$\delta := \frac{1}{N}, \quad x_i := \frac{i}{N} = i\delta, \quad i = 0, \dots, N.$$

We now set $I_N := \{x_0, \dots, x_N\}$ and define A_N to be the set of all functions $u^N : I_N \to \mathbb{R}^2$. Then we parameterize: $u_i^N = u^N(x_i)$ and $v_i^N = v^N(x_i)$. Until now we have seen E_N as a functional defined on the discrete grid, i.e. $E_N : A_N \times A_N \to \mathbb{R}$. But to compute the Γ-limit, we have to embed the domain for all N in a single space. So we identify u^N with

$$\tilde{u}^N(x) := u_i^N + \frac{u_{i+1}^N - u_i^N}{\delta}(x - x_i) \ \text{ if } x \in [x_i, x_{i+1}].$$

Now we assign to $E_N : A_N \times A_N \to \mathbb{R}$ the functional $\widetilde{E}_N : W^{1,p} \times W^{1,p} \to \mathbb{R}$:

$$\widetilde{E}_N(\tilde{u}^N, \tilde{v}^N) = \begin{cases} E_N(u^N, v^N) & \text{if } u^N \in A_N \text{ and } v^N \in A_N \\ +\infty & \text{else.} \end{cases}$$

In the following we will simply write E_N, u^N and v^N instead of $\widetilde{E}_N$, $\tilde{u}^N$ and $\tilde{v}^N$.

2. Compactness

Theorem 2.1. *If the energy of a sequence (u^N, v^N) is bounded, we can take weakly converging subsequences of u^N and v^N. Precisely, if $E_N(u^N, v^N) < C$ for all N and if the boundary values are given by $u^N(0) = P_1$, $v^N(0) = P_2$ then there exists $\bar{u}$, $\bar{v}$ and a subsequence N_j such that $u^{N_j} \rightharpoonup \bar{u}$ and $v^{N_j} \rightharpoonup \bar{v}$ in $W^{1,p}$.*

Proof. The statement follows almost directly from the growth condition:

$$\begin{aligned} C > E_N(u^N, v^N) &\geq \delta \sum_{i=0}^{N-1} V\left(\frac{|u_i^N - u_{i+1}^N|}{\delta} \right) \\ &= \int_0^1 V(|(u^N)'|)\,\mathrm{d}x \\ &\geq c_1 \|(u^N)'\|_{L^p}^p - c_2. \end{aligned}$$

With Poincaré and the weak compactness of $W^{1,p}$ the statement follows for u^N. Repeating the proof using the already extracted subsequence and using v^N instead of u^N completes the proof. □

Theorem 2.2. *From $E_N(u^N, v^N) < C$ for all N it follows that $\|u^N - v^N\|_{L^p} \to 0$.*

Proof. First we define the piecewise constant function $z(x)$ by

$$z^N(x) := u_i^N - v_i^N \quad \text{if } x \in [x_i - \tfrac{\delta}{2}, x_i + \tfrac{\delta}{2}).$$

Using the bound on the energy, we get

$$\begin{aligned} C > E_N(u^N, v^N) &\geq \delta \sum_{i=0}^{N-1} V\left(\frac{|u_i^N - v_i^N|}{\delta}\right) = \delta \sum_{i=0}^{N-1} V\left(\frac{|z^N(x_i)|}{\delta}\right) \\ &= \int_0^1 V\left(\frac{|z^N(x)|}{\delta}\right) \mathrm{d}x \geq c_1 \|\tfrac{z^N}{\delta}\|_{L^p}^p - c_2 \\ &= \frac{c_1}{\delta^p} \|z^N\|_{L^p}^p - c_2. \end{aligned}$$

With $N \to \infty$ (and hence $\delta \to 0$) we get

$$\|z^N\|_{L^p} \to 0. \tag{4}$$

Here z^N is a piecewise constant function, which is equal to $u^N(x) - v^N(x)$ at the points x_i, but for the proof we have to show that the difference between the piecewise affine functions $u^N(x) - v^N(x)$ has to vanish. To shorten things up, we write $w^N(x) := u^N(x) - v^N(x)$. What remains to be shown is that w^N converges to zero in L^p. To do that, we will show the following inequality

$$\int_0^1 |w^N(x)|^p \,\mathrm{d}x \leq \int_0^1 |z^N(x)|^p \,\mathrm{d}x. \tag{5}$$

Now consider the interval $[x_i, x_{i+1}]$ for arbitrary $i \in \{0, \ldots, N-1\}$. There w is affine and the modulus of an affine function is convex. Also because the p-th power of a non-negative and convex C^2 function is again convex, we can (still for $x \in [x_i, x_{i+1}]$)) make the estimate

$$|w^N(x)|^p \leq g(x) := |w^N(x_i)|^p + \frac{|w^N(x_{i+1})|^p - |w^N(x_i)|^p}{\delta}(x - x_i),$$

and that gives us

$$\int_{x_i}^{x_{i+1}} g(x) \,\mathrm{d}x = \frac{1}{2}\delta(|w^N(x_i)|^p + |w^N(x_{i+1})|^p) = \int_{x_i}^{x_{i+1}} |z^N(x)|^p \,\mathrm{d}x.$$

From that follows (5) and with (4) then the claim. □

Remark 2.3.

(i) From Theorem 2.2 we can conclude that both subsequences in Theorem 2.1 indeed converge to the same limit.
(ii) If there exists a u such that $u^N \to u$ in L^p, then without extracting a subsequence we know: $u^N \rightharpoonup u$ in $W^{1,p}$ (and because of Theorem 2.2 also for $v^N \rightharpoonup u$)
(iii) Theorem 2.2 indicates that the Γ-limit of the functional $E_N(u^N, v^N)$ will depend only on one function.

3. The Γ-limit

In this section we want to compute the Γ-limit of the sequence E_N. Γ-convergence was originally introduced in the 70s by De Giorgi [13], [15]. Standard references about this topic include amongst others Dal Maso [12], Braides [7] and Attouch [6].

Let us shortly review the definition and some important properties:

Definition 3.1 (Γ-Convergence). The sequence $F_j : X \to \overline{\mathbb{R}}$ Γ-converges in X to $F_\infty : X \to \overline{\mathbb{R}}$, if for all $x \in X$ the following conditions hold:

(i) (lim inf-inequality)

$$\forall x_j \to x \text{ we have:} \quad F_\infty(x) \le \liminf_{j\to\infty} F_j(x_j). \tag{6}$$

(ii) (existence of a recovery sequence)

$$\forall x \in X\ \exists x_j \to x \text{ with:} \quad F_\infty(x) = \lim_{j\to\infty} F_j(x_j). \tag{7}$$

The function F_∞ is called the Γ-Limit of (F_j) and we write $F_\infty = \Gamma\text{-}\lim_j F_j$.

Remark 3.2. Here we summarize some of the key properties of Γ-convergence:

(i) (convergence of minimizers) Let $F_\infty = \Gamma\text{-}\lim_j F_j$ and let a compact set $K \subset X$ exist such that $\inf_X F_j = \inf_K F_j$ for all j. Then

$$\exists \min_X F_\infty = \lim_{j\to\infty} \inf_X F_j.$$

If (x_j) is a converging sequence with $\lim_j F_j(x_j) = \lim_j \inf_X F_j$, then its limit is a minimum point for F_∞

(ii) (Stability under continuous perturbations) If (F_j) is a sequence of functionals with $F_j \xrightarrow{\Gamma} F_\infty$ and g is a continuous function, then:

$$\Gamma\text{-}\lim_j (F_j + g) = F_\infty + g.$$

In the following theorem we compute the Γ-limit of the sequence of functionals E_N and then extend it in Theorem 3.7 to include a macroscopic distribution φ.

Theorem 3.3. *Let $1 < p < \infty$ and let $V : [0,\infty) \to [0,+\infty)$ be a convex function, which takes its minimum value 0 at the point 1 and fulfills the growth condition*

$$c_1|z|^p - c_2 \le V(z) \le c_3(1 + |z|^p). \tag{8}$$

Take E_N to be the functional given by (1). Then the Γ-limit of E_N with respect to $W^{1,p}([0,1],\mathbb{R}^2)$ with weak topology is given by

$$F(u,v) = \begin{cases} \int_0^1 \psi(|u'(x)|)\,\mathrm{d}x & \text{if } u = v \\ \infty & \text{else} \end{cases}$$

with

$$\psi(z) := \begin{cases} 0 & 0 \le z \le 1 \\ 2V(z) & 1 \le z \le 2 \\ 2V(z) + 2V\left(\frac{z}{2}\right) & 2 \le z. \end{cases}$$

Remark 3.4. Even when we are modeling harmonic springs (i.e., taking a quadratic potential such as $V(z) = (z-1)^2$), the resulting model is clearly nonlinear.

Proof. *Step 1:* First we will show the liminf inequality. By Theorem 2.2 in the case $u \neq v$ both sides of the inequality are infinity and so we only have to consider the case $u = v$. Now we split E_N into three parts in the following way:

$$E_N^1(u^N, v^N) := \delta \sum_{i=0}^{N-1} V\left(\frac{|u_i^N - u_{i+1}^N|}{\delta}\right),$$

which corresponds in integral form to

$$F_N^1(u^N, v^N) := \begin{cases} \int_0^1 V(|(u^N)'(x)|)\,\mathrm{d}x & \text{if } u^N \in A_N \\ +\infty & \text{else.} \end{cases}$$

Define E_N^2 in the same way by replacing u^N with v^N in E_N^1. The remaining functional

$$E_N^3(u^N, v^N) := \delta \sum_{i=0}^{N-1} V\left(\frac{|u_i^N - v_i^N|}{\delta}\right) + V\left(\frac{|u_{i+1}^N - v_i^N|}{\delta}\right)$$

can be seen as only depending on w^N – where $w^N \in A_{2N}$ alternates between the points of u^N and v^N. So

$$(w_0^N, \ldots, w_{2N+1}^N) = (u_0^N, v_0^N, u_1^N, \ldots, v_{N-1}^N, u_N^N, v_N^N),$$

$$E_N^3(w^N) := 2\frac{\delta}{2} \sum_{i=0}^{N-1} V\left(\frac{1}{2}\frac{|w_{2i}^N - w_{2i+1}^N|}{\frac{\delta}{2}}\right) + V\left(\frac{1}{2}\frac{|w_{2i+2}^N - w_{2i+1}^N|}{\frac{\delta}{2}}\right).$$

Keeping in mind that the fineness of the grid is doubled, we can assign the following integral form to E_N^3:

$$F_N^3(u^N, v^N) := F_N^3(w^N) = \begin{cases} \int_0^1 2V\left(\frac{|(w^N)'(x)|}{2}\right)\mathrm{d}x & w^N \in A_{2N} \\ +\infty & \text{else.} \end{cases}$$

Notice that also here we can assume $w^N \to u$ in L^p.
Since an integral functional with convex integrand is weakly lower semi-continuous, the following is true for arbitrary $(u^N, v^N) \rightharpoonup (u,u)$:

$$\begin{aligned}
\liminf_N E_N(u^N,v^N) &\geq \liminf_N E_N^1(u^N,v^N) + \liminf_N E_N^2(u^N,v^N) + \liminf_N E_N^3(u^N,v^N) \\
&= \liminf_N \int_0^1 V(|(u^N)'(x)|)\,\mathrm{d}x + \liminf_N \int_0^1 V(|(v^N)'(x)|)\,\mathrm{d}x \\
&\quad + \liminf_N \int_0^1 2V\left(\frac{|(w^N)'(x)|}{2}\right)\mathrm{d}x \\
&\geq \liminf_N \int_0^1 V^{**}(|(u^N)'(x)|)\,\mathrm{d}x + \liminf_N \int_0^1 V^{**}(|(v^N)'(x)|)\,\mathrm{d}x \\
&\quad + \liminf_N \int_0^1 2V^{**}\left(\frac{|(w^N)'(x)|}{2}\right)\mathrm{d}x \\
&\geq \int_0^1 2V^{**}(|u'(x)|)\,\mathrm{d}x + \int_0^1 2V^{**}(\frac{|u'(x)|}{2})\,\mathrm{d}x \\
&= F(u,u).
\end{aligned}$$

Here $V^{**}(|\cdot|) : \mathbb{R}^2 \to \mathbb{R}$ denotes the two-dimensional convex envelope of $V(|\cdot|) : \mathbb{R}^2 \to \mathbb{R}$, where $V(|\cdot|)$ is seen as a function mapping $\mathbb{R}^2$ to $\mathbb{R}$ that only depends on the modulus. So the envelope is also of that form and defined as

$$V^{**}(|y|) = \max_{f:\mathbb{R}^2\to\mathbb{R} \text{ convex}} \{f(y) : f(x) \leq V(x)\, \forall x \in \mathbb{R}^2\}$$

And since $V(\cdot) : [0,\infty) \to [0,\infty)$ is convex and takes its minimum value 0 at the point 1, we get the following result:

$$V^{**}(|y|) = \begin{cases} 0 & |y| \leq 1 \\ V(|y|) & |y| > 1. \end{cases}$$

Since $\psi(z)$ was defined as

$$\psi(z) = \begin{cases} 0 & 0 \leq z \leq 1 \\ 2V(z) & 1 \leq z \leq 2 \\ 2V(z) + 2V\left(\frac{z}{2}\right) & 2 \leq z, \end{cases}$$

the proof of the lower bound is concluded.

Step 2: It remains to show the lim sup inequality or equivalently the existence of a recovery sequence:

$$\forall u \in W^{1,p}\ \exists (u^N,v^N) \rightharpoonup (u,u) \text{ such that: } \lim_N E_N(u^N,v^N) = F(u).$$

First we restrict u to be affine with derivative ≥ 1 and to simplify notation, we assume that it has the following form:

$$u(x) = (z\cdot x, 0), \qquad u'(x) = (z,0) \text{ for } x \in [0,1].$$

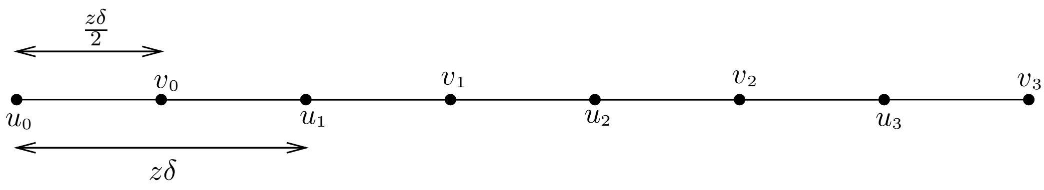

Figure 3.1: The recovery sequences u^N and v^N for $z = 3$

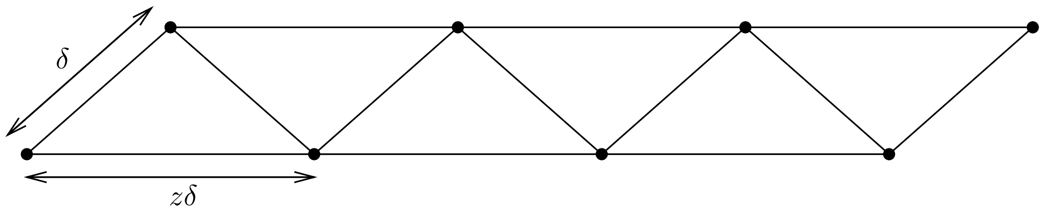

Figure 3.2: The recovery sequences u^N and v^N for $z = 1.5$

We need different recovery sequences for the cases $z > 2$ and $1 \leq z \leq 2$ (see *Step 4* for $0 \leq z < 1$).

Case 1: $[z > 2]$ choose for u^N and v^N (see Figure 3.1):

$$u^N(x_i) = (z \cdot x_i, 0), \qquad v^N(x_i) = \left(z \cdot \left(x_i + \tfrac{\delta}{2}\right), 0\right).$$

Since $\|u^N - u\|_{L^p} = 0$ and $\|v^N - u\|_{L^p} = |z \cdot \frac{\delta}{2}|^p$, both sequences converge in L^p to u. In Theorem 2.1 it was shown that u^N and v^N have a weak limit in $W^{1,p}$ and by the uniqueness of the limit in L^p this limit is equal to u.

$$\begin{aligned} &\lim_N E_N(u^N, v^N) \\ = \;& \lim_N \delta \sum_{i=0}^{N-1} V\left(\frac{|z \cdot \delta|}{\delta}\right) + V\left(\frac{|z \cdot \delta|}{\delta}\right) + V\left(\frac{|z \cdot \frac{\delta}{2}|}{\delta}\right) + V\left(\frac{|z \cdot \frac{\delta}{2}|}{\delta}\right) \\ = \;& \lim_N \delta \sum_{i=0}^{N-1} 2V(z) + 2V\left(\frac{z}{2}\right) \\ = \;& \int_0^1 2V(z) + 2V\left(\frac{z}{2}\right) \,\mathrm{d}x = F(u). \end{aligned}$$

Case 2: $[1 \leq z \leq 2]$ Define the recovery sequence (see Figure 3.2) by

$$u^N(x_i) = \left(z \cdot x_i, -\tfrac{\delta}{4}\sqrt{4 - z^2}\right), \qquad v^N(x_i) = \left(z \cdot \left(x_i + \tfrac{\delta}{2}\right), \tfrac{\delta}{4}\sqrt{4 - z^2}\right).$$

One should notice here that the term $\frac{\delta}{4}\sqrt{4 - z^2}$ was chosen so that $|u_i^N - v_i^N| = \delta$.

The convergence of u^N (and with Theorem 2.2 also of v^N) follows with $\|u^N - u\|_{L^p} =$

$|\frac{\delta}{4}\sqrt{4-z^2}|^p$) in the same way as in *Case 1.*

$$\lim_N E_N(u^N, v^N) = \lim_N \delta \sum_{i=0}^{N-1} V\left(\frac{|z\cdot\delta|}{\delta}\right) + V\left(\frac{|z\cdot\delta|}{\delta}\right) + \underbrace{V\left(\frac{\delta}{\delta}\right)}_{=0,\text{ assumption}} + V\left(\frac{\delta}{\delta}\right)$$

$$= \lim_N \delta \sum_{i=0}^{N-1} 2V(z) = \int_0^1 2V(z)\,\mathrm{d}x = F(u).$$

Note: For the case $[0 \le z \le 1]$ it is possible to construct a realizing sequence by defining a simple folding pattern, that reduces the length of the chain (to be more precise: each folding of a chain with $N = 4$ reduces the length to that of a chain with $N = 2$, but does not change the distances between the mass-points and therefore does not cost any energy). But we will instead deal with this case in *Step 4* of this proof.

Step 3: We now have to make the transition from the affine to the piecewise affine functions with derivatives ≥ 1 (in the following we call the set of all such functions $\widetilde{PA}([0,1],\mathbb{R}^2)$), i.e., consider u to be affine on intervals $[a_j, a_{j+1}]$ with $0 = a_0 < a_1 < \ldots < a_n < a_{n+1} = 1$. In the intervals, where u is affine, we choose the recovery sequences exactly as in *Step 2* of this proof. The only thing to check is that nothing bad happens at the breakpoints. Focusing on one of the finitely many breakpoints with the pair of recovery sequences (u^N, v^N) and $(\tilde{u}^N, \tilde{v}^N)$, we get:

$$\delta\left(V\left(\frac{|u_i^N - \tilde{u}_{i+1}^N|}{\delta}\right) + V\left(\frac{|v_i^N - \tilde{v}_{i+1}^N|}{\delta}\right) V\left(\frac{|u_i^N - v_i^N|}{\delta}\right) + V\left(\frac{|\tilde{u}_{i+1}^N - v_i^N|}{\delta}\right)\right)$$
$$\le \delta \cdot 4C_2 \overset{\delta\to 0}{\to} 0$$

This holds, since by construction the terms $|u_i^N - \tilde{u}_{i+1}^N|$, $|v_i^N - \tilde{v}_{i+1}^N|$ and $|\tilde{u}_{i+1}^N - v_i^N|$ (for sufficiently small δ) are bounded by a constant C_1 and so there exists a $C_2 \in \mathbb{R}$ such that $V(x) \le C_2$ for $x \in [0, C_1]$.

Step 4: To make the final transition to $W^{1,p}$, we use Lemma 3.6 below. To fulfill the assumptions of this lemma, we have to show that $\widetilde{PA}([0,1],\mathbb{R}^2)$ is energy dense in $W^{1,p}$.

But first we put a step in between and show the energy density of $\widetilde{PA}([0,1],\mathbb{R}^2)$ in the set of all piecewise affine functions without any restriction on the derivatives (in the following called $PA([0,1],\mathbb{R}^2)$).

Take an arbitrary $u \in PA([0,1],\mathbb{R}^2)$ and call the intervals where u is affine $[a_j, a_{j+1}]$. To construct u_1, we set $u_1(a_j) = u(a_j)$ and insert for all j, where $|u(a_j) - u(a_{j+1})| < |a_j - a_{j+1}|$, a new point $y_j := \frac{a_j + a_{j+1}}{2}$ into each of those intervals. Then we choose $u_1(y_j)$ to be in the intersection of the two spheres $S(u(a_j), \frac{|a_j - a_{j+1}|}{2})$ and $S(u(a_{j+1}), \frac{|a_j - a_{j+1}|}{2})$. To construct u_k, we now insert $2k-1$ equidistant points (instead of just inserting one point y_j) into every $[a_j, a_{j+1}]$, where the derivative is < 1, and repeat the construction as above. Clearly the distance between u and u_k is bounded by $\frac{|a_j - a_{j+1}|}{2k-1}$ and so we have uniform convergence. From that the convergence of the energy follows directly and by the usual compactness argument we get weak convergence of u_k in $W^{1,p}$.

To complete the density argument, we choose an arbitrary piecewise affine function that converges to u in $W^{1,p}$. So $u_k' \to u'$ in L^p and from that we take an a.e. pointwise converging subsequence.

With Fatou and the continuity of ψ we get:

$$\int_0^1 \psi(|u'(x)|)\,\mathrm{d}x \le \int_0^1 \liminf_k \psi(|u_k'(x)|)\,\mathrm{d}x \le \liminf_k \int_0^1 \psi(|u_k'(x)|)\,\mathrm{d}x.$$

And from the growth condition (8) follows: $G(z) = C(1+z^p) - \psi(z) \ge 0$. Now we apply Fatou on G and together with the L^p-convergence ($\lim_k \int C(1+|u_k'|^p) = \lim_k \int C(1+|u'|^p)$) we get:

$$-\int_0^1 \psi(|u'(x)|)\,\mathrm{d}x \le -\liminf_k \int_0^1 \psi(|u_k'(x)|)\,\mathrm{d}x.$$

It follows $F(u_k) \to F(u)$ and with that the energy density.

In Lemma 3.6 we choose for A a ball in $W^{1,p}$ (i.e. $A = \{x \in W^{1,p} : \|x\|_{1,p} < R\}$) with the norm of L^p and for $B \subset A$ a ball in the subspace of piecewise affine functions. Since we want to find a recovery sequence for any given $u \in W^{1,p}$, we have to choose the radius so that u, the energy dense sequence, and the recovery sequences to the elements of these sequences are contained.

To find the upper bound, we can use the coercivity of the energy: assuming $u_k \to u$ with $F(u_k) \to F(u)$ and $u_k^i \to u_k$ with $E^N(u_k^N) \to F(u_k)$, it follows (for N large enough): $E^N(u_k^N) < F(u_k) + 1 < F(u) + 2$. So $E_N(u_k^N)$ and $E_N(u_k)$ are uniformly bounded from above and with the coercivity also the norms of the derivatives of u_k^N and u_k. With Poincaré we have found a bound C and so we can now set $R = C$, where R was the radius of A.

Applying Lemma 3.6 gives us a recovery sequence that is bounded in $W^{1,p}$ and converges to u in L^p. From the weak compactness of $W^{1,p}$ it follows that the sequence is weakly converging to u in $W^{1,p}$. □

We needed the following definition and lemma in the proof of Theorem 3.3:

Definition 3.5. Let A be a metric space, $B \subset A$ and $F : A \to \mathbb{R}$. B is energy dense in A, if and only if:

$$\forall u \in A\ \exists u_k \in B \text{ such that } \quad u_k \to u \text{ and } F(u_k) \to F(u).$$

Lemma 3.6. *Let A be a metric space, $B \subset A$, $F_i : A \to \mathbb{R}$ and $F : A \to \mathbb{R}$. In addition let B be energy dense in A and assume that*

$$\forall u \in B\ \exists u_i \to u \text{ such that } \quad F_i(u_i) \to F(u). \tag{9}$$

Then we get:

$$\forall u \in A\ \exists u_i \to u \text{ such that } \quad F_i(u_i) \to F(u). \tag{10}$$

Proof. One can obtain the statement by taking an appropriate diagonal subsequence. □

In the following theorem, we will extend our previous result to include the material distribution φ in the energy functional.

Theorem 3.7. *Take the assumptions as in Theorem* 3.3. *But here the energy functional we consider is given by* (3) *with* $\varphi \in C^0([0,1],(0,\infty))$. *Then the* Γ*-Limit is given by*

$$F(u,v) = \begin{cases} \int_0^1 \psi(|u'(x)|)\varphi(x)\,\mathrm{d}x & \text{if } u = v \\ \infty & \text{else} \end{cases}$$

with $\psi(z)$ *as before.*

Proof. 1. If φ is constant, then the statement is true by Theorem 3.3.

2. Now we have to extend the result to piecewise constant φ, i.e.,

$$\varphi(x) = \sum_{j=0}^{n} c_j \chi_{[a_j,a_{j+1}]}(x), \quad c_j \in \mathbb{R},\ 0 = a_0 < a_1 < \ldots < a_n = a_{n+1} = 1,$$

$$E_N^j(u^N, v^N) = \delta \sum_{\substack{i=0 \\ a_j \le x_i < a_j+1}}^{N-1} \varphi(x_i) \left(V\left(\frac{|u_i^N - u_{i+1}^N|}{\delta} \right) + \ldots \right).$$

We already know from 1. that

$$\Gamma - \lim E_N^j(u^N, v^N) = F^j(u) = \int_{a_j}^{a_{j+1}} \psi(|u'(x)|)c_j\,\mathrm{d}x. \tag{11}$$

So it remains to show

$$\Gamma - \lim E_N(u^N, v^N) = \Gamma - \lim \sum_{j=0}^{n} E_N^j(u^N, v^N) = \sum_{j=0}^{n} F^j(u). \tag{12}$$

The liminf inequality follows from the subadditivity:

$$\begin{aligned} \forall (u^N, v^N) \rightharpoonup (u,u) \quad \liminf_N \sum_{j=0}^{n} E_N^j(u^N, v^N) &\ge \sum_{j=0}^{n} \liminf_N E_N^j(u^N, v^N) \\ &\overset{(11)}{\ge} \sum_{j=0}^{n} F^j(u). \end{aligned}$$

To show the lim sup inequality, one has to put together the recovery sequences on the intervals $[a_j, a_{j+1}]$. This works similar to *Step 3* in the proof of Theorem 3.3. This proofs (12).

3. Now let φ be C^0 and choose a sequence of piecewise constant φ_ϵ so that for arbitrary $\epsilon > 0$

$$\varphi_\epsilon \to \varphi \text{ in } L^\infty \quad \text{and} \quad F_\epsilon(u) := \int_0^1 \psi(|u'(x)|)\varphi_\epsilon(x)\,\mathrm{d}x \leq F(u) + \epsilon. \tag{13}$$

The latter is valid, since we get from uniform convergences that $F_\epsilon(u) \to F(u)$.
Let $u \in W^{1,p}$ now be arbitrary and choose (by *Step 2*) the recovery sequences $(u_\epsilon^N, v_\epsilon^N) \rightharpoonup (u, u)$ so that

$$\begin{aligned} E_N^\epsilon(u_\epsilon^N, v_\epsilon^N) &:= \delta \sum_{i=0}^{N-1} \varphi_\epsilon(x_i) \left(V\left(\frac{|(u_\epsilon^N)_i - (u_\epsilon^N)_{i+1}|}{\delta} \right) + \ldots \right) \\ &\leq F_\epsilon(u) \overset{(13)}{\leq} F(u) + \epsilon. \end{aligned}$$

After taking a diagonal sequence, the lim sup inequality follows with $\epsilon \to 0$.

It remains to be shown that the liminf inequality holds for all $(u^N, v^N) \to (u, u)$. So we choose a sequence of piecewise constant φ_ϵ with:

$$\varphi_\epsilon \leq \varphi, \qquad \varphi_\epsilon \to \varphi \text{ in } L^\infty \quad \text{and} \quad F_\epsilon(u) \geq F(u) - \epsilon. \tag{14}$$

This leads to

$$\liminf_N E_N(u^N, v^N) \geq \liminf_N E_N^\epsilon(u^N, v^N) \geq F_\epsilon(u) \overset{(14)}{\geq} F(u) - \epsilon.$$

Together with $\epsilon \to 0$ this concludes the proof. □

4. Application to shape optimization

4.1. Deformation

Before we can come to the shape-optimization problem, we have to find a way to compute the deformation for a given load, i.e., to minimize

$$F(u) = \int_0^1 \psi(|u'(x)|)\varphi(x) - f(x)u(x)\,\mathrm{d}x$$

with $f : [0,1] \to \mathbb{R}^2 \in W^{-1,p}$ and where V and ψ are as in Theorem 3.3. Since ψ is not strictly convex we cannot expect a unique minimizer. So we add a small strictly convex term:

$$\tilde{\psi}(z) := \begin{cases} \frac{1}{N}|z|^2 & 0 \leq z \leq 1 \\ 2V(z) + \frac{1}{N}|z|^2 & 1 \leq z \leq 2 \\ 2V(z) + 2V\left(\frac{z}{2}\right) + \frac{1}{N}|z|^2 & 2 \leq z. \end{cases}$$

To numerically solve the minimization problem, we have to discretize it first (i.e. approximate u by a linear combination of some base functions and using a quadrature formula to replace the integrals). Notice here that the choice of the grid-fineness is not already given by the problem statement, but can be chosen so that we have a sufficiently good approximation.

What follows is a short summary of the numerical algorithm used:

1. Fix an initial point u_0, e.g., the reference configuration.
2. Compute the gradient in u_0 and use $-\nabla I[u_0]$ as search direction (note: in our case, it is relatively easy to compute an explicit formulation of the derivative). So the problem was reduced to an 1-dimensional minimization: Find $t \in \mathbb{R}$ such that $I[u_0 - t\nabla I[u_0]]$ is minimal.
3. Find the interval $[a, b]$, in which the optimal t is.
4. Use golden section search (see e.g. Section 6.1.1 in Jarre and Stoer [17]) on the functional $I[u_0 - t\nabla I[u_0]]$ in the interval $[a, b]$ to compute the minimizer t_0.
5. Set: $u_1 = u_0 - t_0\nabla I[u_0]$.

Now use u_1 in *Steps 2–4* and compute u_2 as in *Step 5*. Repeat this steps until an approximated limit of the sequence u_k is achieved.

4.2. Shape Optimization

Now we are looking for the minimizer of the functional $J[\varphi] : C^0([0, 1], (0, \infty)) \to \mathbb{R}$ restricted to the set $\{\varphi \in C^0([0, 1], (0, \infty)) : \int_0^1 \varphi \,\mathrm{d}x = 1\}$, where J is defined as:

$$J[\varphi] = \sum_{k=1}^{L} \lambda_k \|\operatorname*{argmin}_u F(u, f_k, \varphi)\|.$$

$F(u, f_k, \varphi)$ is the Γ-limit as in Section 4.1 with the force f_k, and λ_k is the probability that f_k is present. Here f_k has the form:

$$f_k^{(1)}(x) = \sum a_j^{(1)} \delta_{x_j}(x),$$

$$f_k^{(2)}(x) = \sum a_j^{(2)} \delta_{x_j}(x).$$

$a_j^{(1)}$, $a_j^{(2)} \in \mathbb{R}$, $f_k^{(1)}$ and $f_k^{(2)}$ are the x- and y-components of the force, and $\delta_{x_j}(x) = 1$ if $x = x_j$ and 0 otherwise.

Remark 4.1. Here we use Remark 3.2 (Stability of the Γ-limit under continuous perturbations), since our force terms are continuous as functions from $W^{1,p}$ weak to $\mathbb{R}$ (see e.g. [9, Section 2.1]).

To solve the problem numerically, we have to discretize the functional as in 4.1. Here φ will be approximated by a piecewise constant function on a grid with fineness $\frac{1}{M}$, i.e. we identify φ with a vector in $\mathbb{R}^M$. Since the forces are distributional, they should apply on the grid-points and so, to make things easier, we want the grid of φ to be included in the grid of u (i.e. M is a divisor of $N - 1$).

As before we have to solve a multidimensional optimization problem, but this time there are linear restrictions and the gradient of the functional is not easy to compute. To deal with the restrictions, we use a projection to rewrite the problem:

$$\min_{\varphi \in R} J[\varphi] = \min_{z \in \mathbb{R}^{M-1}} \underbrace{J[w + Zz]}_{=:D[z]},$$

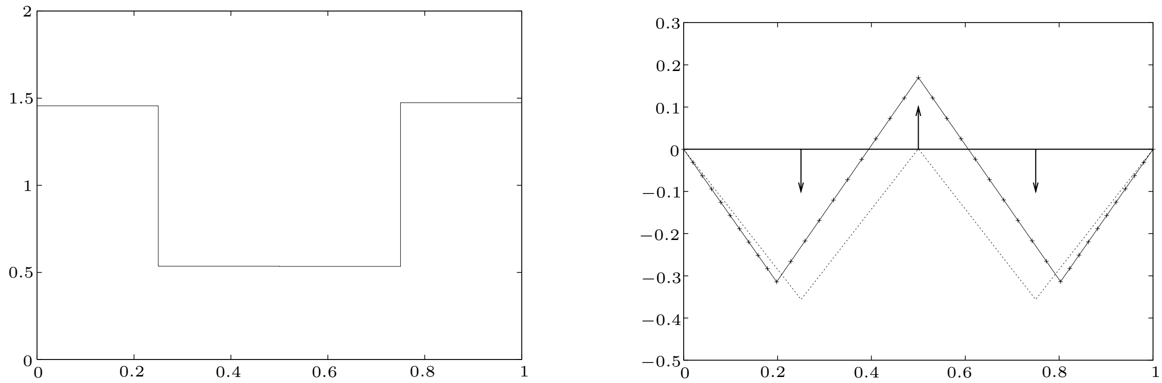

(a) the optimal mass distribution φ

(b) the solid line is u using the optimal φ, the dotted line the u with $\varphi \equiv 1$ and the arrows illustrate f

Figure 4.1: The result of the optimization with respect to Norm I in Example 4.2

where

$$R := \{\varphi \in \mathbb{R}^M : \underbrace{(1, \ldots, 1)}_{:=A} \varphi = M\}$$

is the restricted set, w a specific solution (here: $w = (1, \ldots, 1)$) and Z a null space matrix (i.e. a matrix with $\operatorname{kern} A = \operatorname{im} Z$, see [4] for details). In our case, we have:

$$D[z] = J[1 - z_1 - \ldots - z_M, 1 + z_1, \ldots, 1 + z_M].$$

Now we just have to solve an optimization problem on $\mathbb{R}^{N-1}$ without having an explicit gradient. We use the algorithm of Nelder and Mead, which is based on the following idea: Start with setting up a simplex in the search space and then reflect (in a certain way) the corner with the highest function value with respect to the opposite side (or more precisely: the balance point of the remaining corners) to move step by step to a region with lower values. For a detailed description of this algorithm, see Section 10.3 in *Numerical Recipes in C* [18] or see W. Alt [4].

4.3. Examples

Now we want to use the algorithm to optimize φ with respect to a norm. There are several canonical choices like compliance or displacement. We will discuss the latter (though the results for compliance are similar)

I)

$$\|u - u_0\|_{L^2} = \left(\int_0^1 |u(x) - u_0(x)|^2 \right)^{\frac{1}{2}},$$

II)

$$\|\nabla u\|_{L^\infty} = \operatorname*{ess\,sup}_{[0,1]} \{|\nabla u(x)|\}.$$

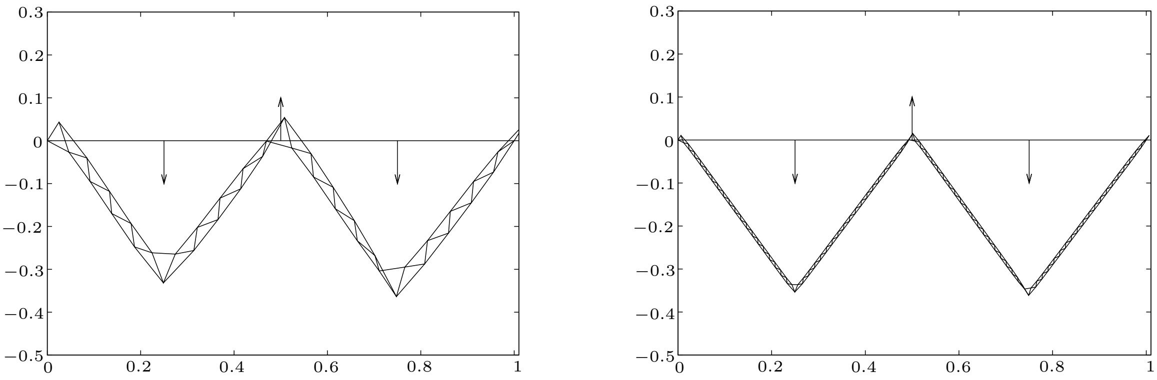

(a) discrete u computed with $N = 20$

(b) discrete u computed with $N = 80$

Figure 4.2: Computing the deformation using the discrete energy functional and the force from Example 4.2

For the numerical computations we have to choose a specific potential, which in all the following examples will be $V(z) = (z-1)^2$ with $z \in \mathbb{R}^+$. We also set $u_0 \equiv 0$ (for Norm I) in this section.

Example 4.2. This example shows that optimization with respect to each norm results in completely different φ's. The force is given by (see Figure 4.1 for a scaled illustration):

$$f^{(2)} = -5\delta_{\frac{1}{4}}(x) + 5\delta_{\frac{1}{2}}(x) - 5\delta_{\frac{3}{4}}(x).$$

The resulting mass distributions are very different for Norm I and II: for Norm I (see Figure 4.1) it is better to strengthen the sides to move the construction up, because the norm adds the squares of the distances between all the points in the deformed and the reference configuration - so it is optimal to decrease the big distances despite at the same time increasing some small ones. For Norm II an even distribution ($\varphi \equiv 1$) is optimal, since the distances between all points are constant and the norm sees only the biggest elongation.

As a comparison, we can also compute the deformation directly with the discrete energy functional (1) using the same algorithm as before. The result (with $\phi \equiv 1$) can be seen in Figure 4.2 and is, even for low N, already very close to the result derived by minimizing the Γ-limit.

Example 4.3. In the case of compression the discrete problem does not have a unique solution and unlike the Γ-limit no straightforward regularization. That means the algorithm will reach a seemingly arbitrary local minimum (of course dependend on the algorithm, the initial configuration, boundary conditions and the force term). We demonstrate this with two very similar forces

$$f^{(1)} = 3\delta_{\frac{1}{4}}(x) - 3\delta_{\frac{3}{4}}(x).$$

and

$$\overline{f}^{(1)} = 3.1\delta_{\frac{1}{4}}(x) - 3.1\delta_{\frac{3}{4}}(x).$$

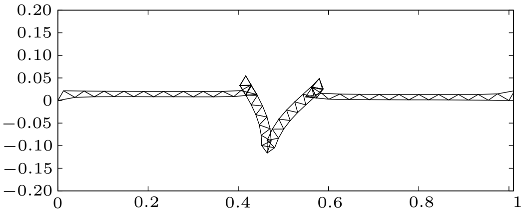

(a) discrete u with respect to f

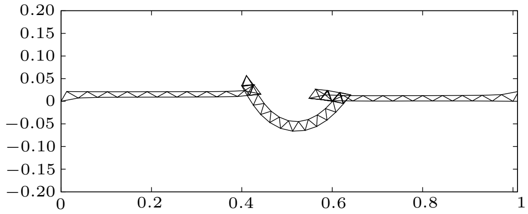

(b) discrete u with respect to $\overline{f}$

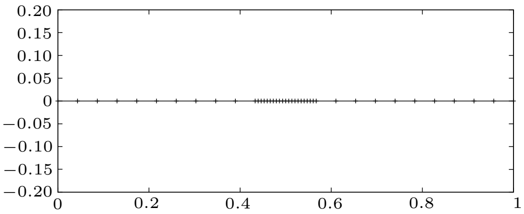

(c) continuous u with respect to f

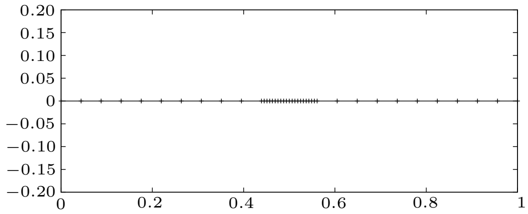

(d) continuous u with respect to $\overline{f}$

Figure 4.3: Comparison of the deformation using the discrete energy (1) and the Γ-limit with forces from Example 4.3

As expected, the result for the discrete problem is not stable, i.e., the small change in the force term causes a large change in u (see Figure 4.3).

In Example 4.2 we have only looked at a single force, but the problem statement was more general and allows multiple forces with a probability distribution. So in the following examples we will consider two forces, both with 50% probability ($\lambda_i = 0.5$). In particular we want to compare, what happens if we are averaging $\|\mathrm{argmin}_u F(u, f_k, \varphi)\|$ or if we take the average of the forces before, i.e:

1. Averaging of $\|\mathrm{argmin}_u F(u, f_k, \varphi)\|$ (hereafter called Problem A):

$$J[\varphi] = \sum_{k=1}^{L} \lambda_k \|\underset{u}{\mathrm{argmin}}\, F(u, f_k, \varphi)\|.$$

2. Averaging the forces (Problem B):

$$\widetilde{J}[\varphi] = \left\| \underset{u}{\mathrm{argmin}}\, F\left(u, \sum_{k=1}^{L} \lambda_k f_k, \varphi\right) \right\|.$$

Example 4.4. Consider the two forces:

$$f_1^{(2)} = -5\delta_{\frac{1}{4}}(x) - 2\delta_{\frac{1}{2}}(x) - 5\delta_{\frac{3}{4}}(x),$$
$$f_2^{(2)} = 5\delta_{\frac{1}{4}}(x) - 2\delta_{\frac{1}{2}}(x) + 5\delta_{\frac{3}{4}}(x).$$

In Problem 2, we use the averaged force instead:

$$\frac{f_1 + f_2}{2} = -2\delta_{\frac{1}{2}}(x).$$

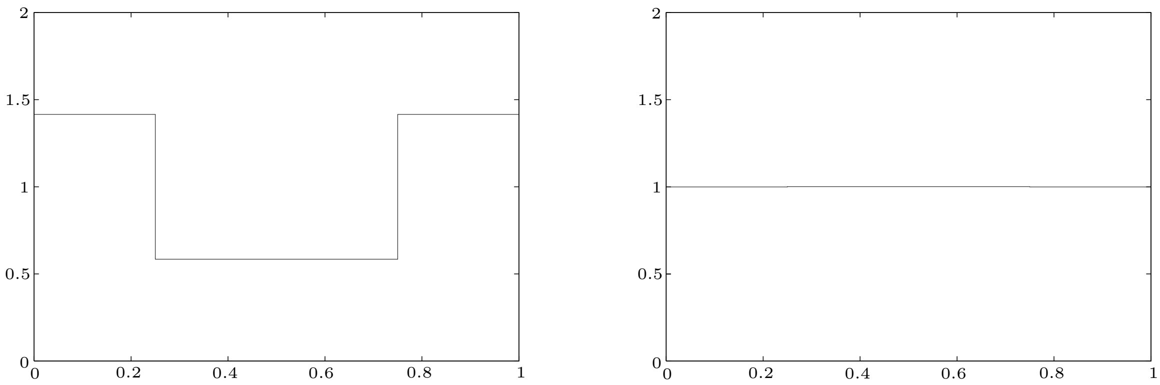

(a) with respect to Problem A

(b) with respect to Problem B

Figure 4.4: The result of the optimization in Example 4.4

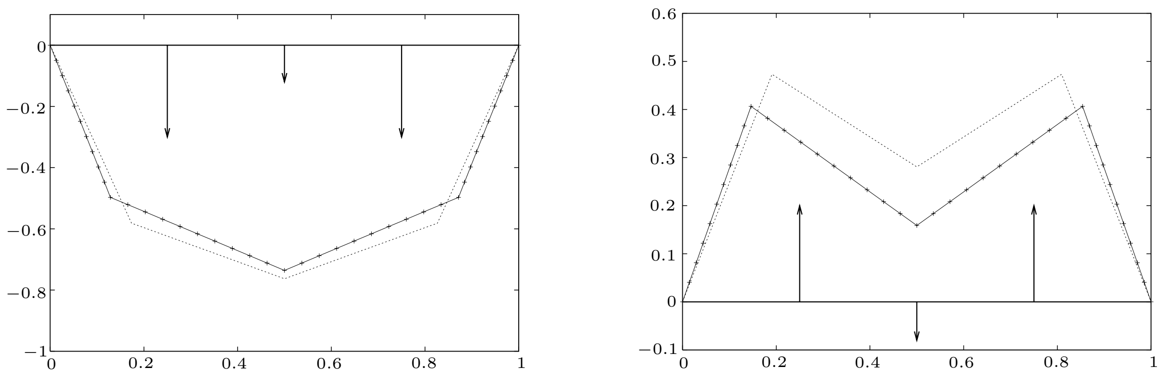

(a) u with respect to the force f_1

(b) u with respect to the force f_2

Figure 4.5: The result of the optimization in Example 4.4

The results with respect to Norm II are shown in Figure 4.4 and 4.5.

While it was optimal with regard to both forces to reinforce the sides, this is not true for the averaged force. This clearly shows that averaging and optimizing is not commutative.

Another option is to compute φ_k for each f_k and then to average these:

$$\varphi = \sum_{k=1}^{L} \lambda_k \underbrace{\underset{\varphi}{\operatorname{argmin}} \| \underset{u}{\operatorname{argmin}} F(u, f_k, \varphi) \|}_{:=\varphi_k} .$$

In a lot of cases this comes close to the result from Method A, e.g. for the following example:

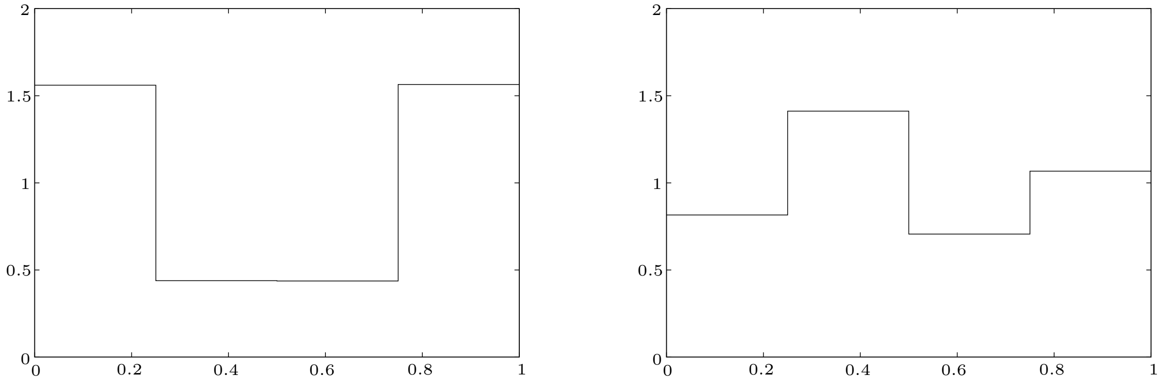

(a) φ_1 (b) φ_2

Figure 4.6: The result of the optimization with respect to f_1 and f_2 in Example 4.5

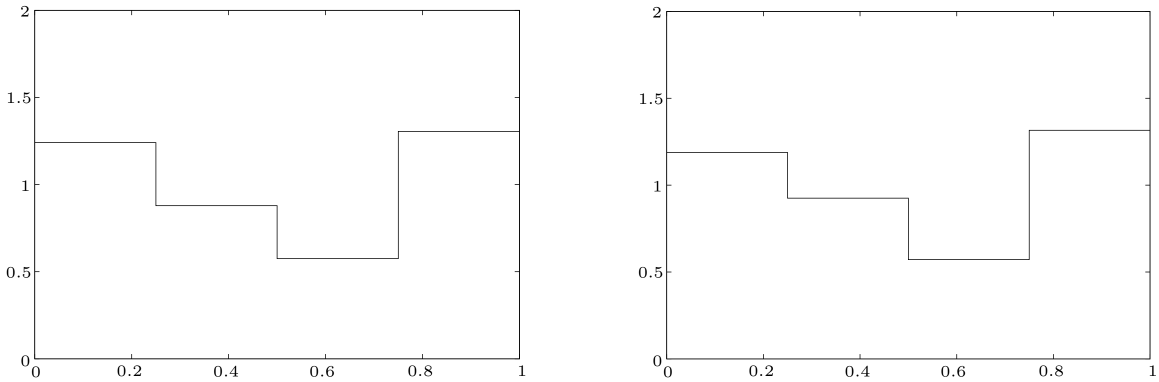

(a) $\frac{\varphi_1+\varphi_2}{2}$ (b) $\operatorname{argmin}_\varphi J[\varphi]$

Figure 4.7: Comparison of the averaged φ with the minimizer of $J[\varphi]$ in Example 4.5

Example 4.5. Consider the forces

$$\begin{aligned} f_1^{(2)} &= -5\delta_{\frac{1}{4}}(x) - 1\delta_{\frac{1}{2}}(x) - 5\delta_{\frac{3}{4}}(x), \\ f_2^{(2)} &= -6\delta_{\frac{1}{4}}(x) + 7\delta_{\frac{1}{2}}(x) - 3\delta_{\frac{3}{4}}(x). \end{aligned}$$

The result of averaging the φ's is very similar to the result from Method A (with respect to Norm I, see Figures 4.6 and 4.7 – but the statement hold true also with respect to Norm II).

The following example will show that this is not true in general:

Example 4.6. Consider the forces:

$$\begin{aligned} f_1^{(1)} &= 4\delta_{\frac{1}{4}}(x), \qquad & f_1^{(2)} &= -1\delta_{\frac{1}{4}}(x), \\ f_2^{(1)} &= 3\delta_{\frac{3}{4}}(x), \qquad & f_2^{(2)} &= -1\delta_{\frac{3}{4}}(x). \end{aligned}$$

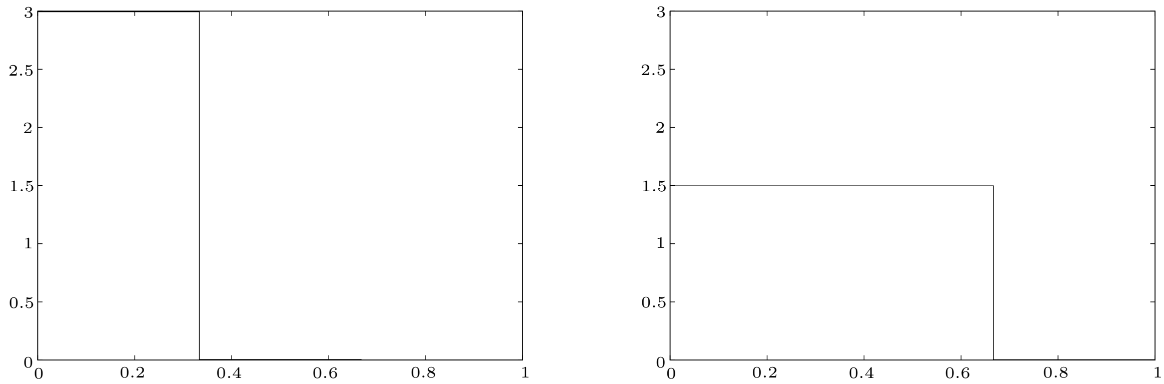

(a) φ_1 (b) φ_2

Figure 4.8: Result of the optimization with respect to f_1 and f_2 in Example 4.6

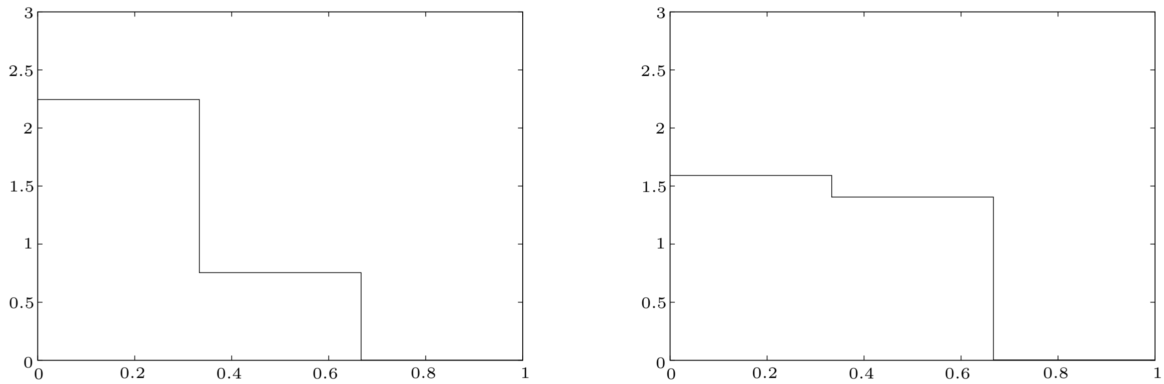

(a) $\frac{\varphi_1+\varphi_2}{2}$ (b) $\operatorname{argmin}_\varphi J[\varphi]$

Figure 4.9: Comparison of the averaged φ with the minimum of $J[\varphi]$ in Example 4.6

and compute (with respect to Norm II):

$$\varphi_1 = \operatorname*{argmin}_{\varphi} \|\operatorname*{argmin}_{u} F(u, f_1, \varphi)\|$$

$$\varphi_2 = \operatorname*{argmin}_{\varphi} \|\operatorname*{argmin}_{u} F(u, f_2, \varphi)\|$$

The results are shown in Figure 4.8. One can clearly see that in both cases nearly the whole mass was distributed in the area that was under strong load.

As one can see in Figure 4.9, the averaged φ in not even close to optimal, since it makes the middle area too weak, so that f_2 causes such a strong deformation, that the advantage with respect to force f_1 does not compensate.

Acknowledgements. The research presented here was done in the framework of a Diplomarbeit (masters thesis) proposed and supervised by Prof. S. Conti at the University of Duisburg-Essen, to whom I am indebted for his invaluable advise and support.

References

[1] G. Allaire: Shape Optimization by the Homogenization Method, Springer, New York (2002).

[2] G. Allaire, E. Bonnetier, G. Francfort, F. Jouve: Shape optimization by the homogenization method, Numer. Math. 76 (1997) 27–68.

[3] G. Allaire, F. Jouve: A level-set method for vibration and multiple loads structural optimization, Comput. Methods Appl. Mech. Eng. 194 (2005) 3269–3290.

[4] W. Alt: Nichtlineare Optimierung, Vieweg, Braunschweig (2002).

[5] F. Alvarez, M. Carrasco: Minimization of the expected compliance as an alternative approach to multiload truss optimization, Struct. Multidiscip. Optim. 29 (2005) 470–476.

[6] H. Attouch: Variational Convergence for Functions and Operators, Pitman, Boston (1984).

[7] A. Braides: Γ-Convergence for Beginners, Oxford University Press, Oxford (2002).

[8] D. Bucur, G. Buttazzo: Variational Methods in Shape Optimization Problems, Progress in Nonlinear Differential Equations 65, Birkhäuser, Basel (2005).

[9] G. Buttazzo, M. Giaquinta, S. Hildebrandt: One-dimensional Variational Problems, Oxford University Press, Oxford (1998).

[10] D. Cioranescu, P. Donato: An Introduction to Homogenization, Oxford University Press, Oxford (1999).

[11] S. Conti, H. Held, M. Pach, M. Rumpf, R. Schultz: Shape optimization under uncertainty a stochastic programming perspective, SIAM J. Optim. 19 (2009) 1610–1632.

[12] G. Dal Maso: An Introduction to Γ-Convergence, Birkhäuser, Boston (1993).

[13] E. De Giorgi: Sulla convergenza di alcune successioni d'integrali del tipo dell'area, Rend. Mat., VI. Ser. 8 (1975) 277–294.

[14] G. Friesecke, R. D. James: A scheme for the passage from atomic to continuum theory for thin films, nanotubes and nanorods, J. Mech. Phys. Solids 48(6–7) (2000) 1519–1540.

[15] E. D. Giorgi, T. Franzoni: Su un tipo di convergenza variazionale, Atti Accad. Naz. Lincei, VIII. Ser., Rend., Cl. Sci. Fis. Mat. Nat. 58 (1975) 842–850.

[16] J. M. Guedes, H. C. Rodrigues, M. P. Bendsøe: A material optimization model to approximate energy bounds for cellular materials under multiload conditions, Struct. Multidiscip. Optim. 25 (2003) 446–452.

[17] F. Jarre, J. Stoer: Optimierung, Springer, Berlin (2003).

[18] W. H. Press, S. A. Teukolsky, W. T. Vetterling, B. P. Flannery: Numerical Recipes in C, 2nd Ed., Cambridge University Press, Cambridge (1992).